3J1-3

Multi-frequency Tissue Characterization of Skin Tissues for Quantitative Ultrasound Diagnosis of Lymphedema

リンパ浮腫の超音波定量診断に向けた複数周波数による皮膚組織の性状解析

Masaaki Omura[1†], Kenji Yoshida[2], Tamaki Honda[1], Shinsuke Akita[3], Ichiro Manabe[3], and Tadashi Yamaguchi[2*] ([1]Grad. School Sci. Eng., Chiba Univ.; [2]Center for Frontier Medical Engineering, Chiba Univ.; [3] Grad. School Med., Chiba Univ.)

大村 眞朗[1†], 吉田 憲司[2], 本田 瑶季[1], 秋田 新介[3], 真鍋 一郎[3], 山口 匡[2*]

([1] 千葉大院 融合理工, [2] 千葉大 CFME, [3] 千葉大院 医)

1. Introduction

This study aims to develop quantitative ultrasound method for diagnosing tissue properties such as a fibrosis and an inflammation of a lymphedema (LE).

Collagen fibers are among the most dominant scatterers in a skin dermis, so the characteristics of echo signals from normal or abnormal tissues may reflect physical properties and acoustic properties of collagen fibers. We have verified the analysis method of the echo amplitude envelope compared between the echo simulation from the histopathological model of collagen fibers and the actual measurement [1].

In this study, the analysis method of the backscattered radio-frequency (RF) signals in the frequency domain was applied to assess the frequency dependence of the backscatter coefficient (BSC) in normal or abnormal skin tissues. Moreover, to confirm the difference of acoustic properties, we analyzed acoustic impedance using scanning acoustic microscopy and 80 MHz transducer.

2. Materials and Methods

2.1 Human samples

The targets were non-diseased LE [LE (-)] (n=3) and diseased LE [LE (+)] (n=3), and each sample was excised from an abdomen and a thigh of women patients, respectively. Each ex vivo skin sample was embedded within 3 wt% low-melting agarose (Agarose super LM, Nacalai tesque) at 40℃. After coagulation, the agarose phantom was sunk in the degassed water at 20℃.

2.2 Analysis of backscattered RF echo signals

RF echo signals were acquired in three-dimension using laboratory-made scanner and 5 kinds of the single element transducers (**Table I**), and were digitized to 12-bits with the sampling frequency of 250 MHz. The focus depth was fixed at the middle layer of the dermis of each sample.

Table I Properties of each transducer

Transducer	F #	Focus depth [mm]	-6dB bandwidth [MHz]
V326 (Panametrics)	5	50.8	3.0-7.0
V328 (Panametrics)	2	19.3	7.0-18.8
PT25 (Toray)	2	10.3	19.1-37.0
PT35 (Toray)	2	10.3	23.4-47.0
PT50 (Toray)	2	10.2	22.9-54.4

In calculation of the BSC, we applied the reflector method [2] using an acrylic board, and compensated attenuation of tissues [3]. The BSC was calculated as

$$BSC(f,d) = 2.17\frac{\gamma^2 F^2}{A_0 \Delta x}\frac{S(f,d)}{S_{ref}(f,d)}A(f,d). \quad (1)$$

In Eq. (1), S and S_{ref} are power spectrum of the measured and acrylic board signal at frequency f and depth position d respectively. The first term means the beam diffraction correction function; reflection coefficient γ of a reflector, aperture area A_0, focus depth F, and length of an analysis window Δx. Attenuation compensation function $A(f,d)$ is defined as Eq. (2)

$$A(f) = e^{4\alpha_0 f x}\left(\frac{2\alpha_0 f \Delta x}{1-e^{-2\alpha_0 f \Delta x}}\right)^2\left\{1+\left(\frac{2\alpha_0 f \Delta x}{2\pi}\right)^2\right\}^2, \quad (2)$$

where α_0 is attenuation coefficient of a tissue, x is the distance between the surface of a tissue and the top of an analysis window. α_0 of 2.0 dB/(mm·MHz) [4] was applied as attenuation coefficient of a skin tissue.

Considered the variance of the sound field and the signal-to-noise ratio, the analysis region for the depth direction was limited among focus depth ± 1.5 mm in each transducer. This distance equaled from an epidermis to a junction between a dermis and a hypodermis, and the power of the envelope was higher than -20 dB bandwidth in measuring an acrylic board. In this analysis region, the voxel of an analysis window that area was 1 mm^3, was shifted in 3-dimension with 50% of overlap.

[†]m.omura@chiba-u.jp, *yamaguchi@faculty.chiba-u.jp

2.3 Analysis of acoustic impedance

To obtain the acoustic properties of each skin tissue, RF echo signals were also measured using scanning acoustic microscopy (modified AMS-50 SI, Honda electronics) with a transducer with the center frequency of 80 MHz. Observed RF echo signals were digitized to 8-bits with the sampling frequency of 2 GHz.

Soon after the experiment of Sect. 2.2, each cross-sectional skin sample was mounted on a polystyrene dish, and RF echo signals from the cross-sectional tissue were acquired via purified water and polystyrene dish. The acoustic impedance was computed in Eq. (3)

$$Z = Z_p\left(1-\frac{P}{P_w}\frac{Z_p-Z_w}{Z_p+Z_w}\right)\Big/\left(1+\frac{P}{P_w}\frac{Z_p-Z_w}{Z_p+Z_w}\right), \quad (3)$$

where P and P_w are the negative peak of RF signals from the boundary of the polystyrene dish - tissue, and that of the purified water - polystyrene dish, respectively. The acoustic impedance of the polystyrene dish Z_p and purified water Z_w were 2.4 MRayl and 1.5 MRayl, respectively.

3. Results

Figure 1 shows the median and 25-75 percentiles of BSCs in this study and in previous study [4]. All BSCs linearly increased with increasing frequency of ultrasound as shown in Fig. 1. Also, the BSC of LE (+) was constantly lower than that of LE (-) regardless of different frequency bandwidth.

Figures 2(a) and **2(b)** display an example of the spatial distribution in LE (-) and LE (+), respectively. **Figs. 2(a-1)** and **2(b-1)** are log-compressed amplitude envelope images at 15 MHz, **Figs. 2(a-2)** and **2(b-2)** are corresponding parametric images of the logarithmic integrated BSC, and **Figs. 2(a-3)** and **2(b-3)** are acoustic impedance maps at 80 MHz. The integrated BSC was calculated at the frequency bandwidth between 9 and 19 MHZ. Spatial distributions for both integrated BSC and acoustic impedance map, the parameters of LE (+) are averagely lower than that of LE (-). Moreover, the boundary between the dermis and the hypodermis is uncertain in the echo amplitude image

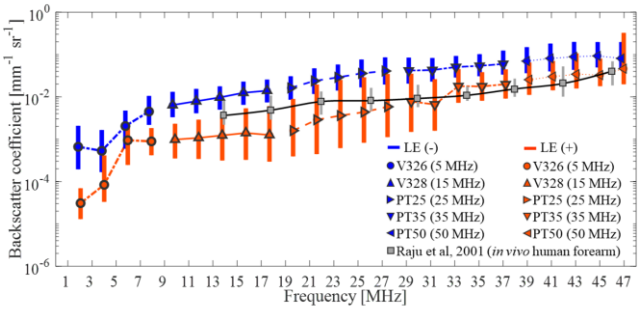

Fig. 1 Evaluated BSCs at 1-47 MHz

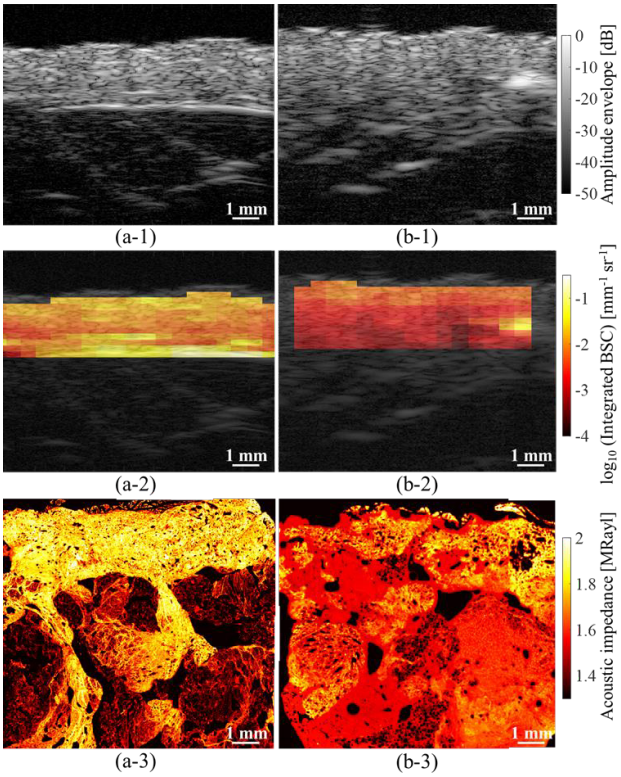

Fig. 2 Example of spatial distributions in LE (-) (a) and LE(+) (b).

of LE (+). As compared to the acoustic impedance maps, its distribution has no contrasts of acoustic impedance in the boundary of LE (+). The properties of the echo amplitude envelope images and the backscattered echo signals can be comparable to the cross-sectional distribution of acoustic impedance.

4. Conclusion

The BSC of the diseased LE was lower at any frequency bandwidth than that of the non-diseased LE. This difference of backscattering properties could be comparable to the difference of the acoustic impedance at 80 MHz. In future works, the relationship among backscattering properties, acoustic properties, and histopathological evaluations will be evaluated.

Acknowledgment

This work was partly supported by JSPS Core-to-Core Program (A. Advanced Research Networks), and KAKENHI Grant Numbers 15H03030, 17H05280, JP17J07762, and the Institute for Global Prominent Research at Chiba University.

References

1. M. Omura et al.: Jpn. J. Appl. Phys. **57** (2018).
2. X. Chen et al.: IEEE Trans. Ultrason. Ferroelectr. Freq. Control **44** (1997).
3. M. L. Oelze et al.: J. Acoust. Soc. Am. **111** (2002).
4. B. I. Raju et al.: Ultrasound Med. Biol. **27** (2001).